[34] Ericsson, L. E., "Universal Scaling Laws for Hypersonic Nose Bluntness Effects," *AIAA Journal*, Vol. 7, No. 12, Dec. 1969, pp. 2222–2227.

[35] Nelson, R. L., "Measurement of Aerodynamic Characteristics of Reentry Configurations in Free Flight at Hypersonic and Near-Orbital Speeds," AGARD Rept. 380, July 1961.

[36] Nelson, R. L., "The Motions of Rolling Symmetrical Vehicles Referred to a Body Axis System," TN 3737, 1956, NACA.

[37] Kanno, J. S., "Spin Induced Forced Resonant Behavior of a Ballistic Body Reentering the Atmosphere," Rept. LMSD-238139, Vol. 3, Jan. 1960, Lockheed Missiles & Space Div., Sunnyvale, Calif.

[38] Pettus, J. J., "Persistent Re-Entry Vehicle Roll Resonance," AIAA Paper 66-49, New York, N.Y., 1966.

[39] Price, D. A., Jr., "Sources, Mechanisms, and Control of Roll Resonance Phenomena for Sounding Rockets," *Journal of Spacecraft and Rockets*, Vol. 4, No. 11, Nov. 1967, pp. 1516–1525.

[40] Price, D. A., Jr. and Ericsson, L. E., "A New Treatment of Roll Pitch Coupling for Ballistic Reentry Vehicles," *AIAA Journal*, Vol. 8, No. 9, Sept. 1970, pp. 1608–1615.

[41] Ericsson, L. E., "Transition Effects on Slender Vehicle Stability and Trim Characteristics," AIAA Paper 73-126, Washington, D.C., 1973.

JANUARY 1974 J. SPACECRAFT VOL. 11, NO. 1

Experimental Wake Flow Properties of a Viking '75 Entry Vehicle

JAMES F. CAMPBELL* AND CLARENCE A. BROWN JR.†
NASA Langley Research Center, Hampton, Va.

An experimental investigation has been conducted to obtain the flow properties in the wake of a model of the blunt Viking '75 entry vehicle. Data are presented for the model at several angles of attack at freestream Mach numbers from 0.2 to 3.95. The characteristics of the wake flowfield are discussed and results are shown to demonstrate the significant variation of wake centerline flow properties in the transonic speed range, the shift in wake profiles with change in angle of attack, and the similarity exhibited by the velocity profiles across the wake.

Nomenclature

b = value of z that corresponds to $(V_\infty - V_1)/(V_\infty - V_{1CL}) = 0.50$
D = maximum diameter of model of Viking entry vehicle
M = Mach number
q = dynamic pressure
V = velocity
X, Y, Z = inertial axis system
x, y, z = distances along X, Y, Z axes
α = angle of attack of model centerline

Subscripts
1 = local flow property
CL = property value on wake centerline
∞ = freestream flow property
stag = value at wake stagnation point

Introduction

NASA'S goals of planetary exploration have resulted in a program to land an unmanned, instrumented payload on Mars. This program has been designated as Viking '75 and is scheduled to commence with a launch in mid-1975 for an encounter with Mars in mid-1976. Research on the atmospheric properties of Mars have indicated the surface pressure to be on the order of 5–10 mbars, a thin atmosphere compared to our Earth's surface pressure of about 1000 mbars. Because of this low pressure, the unmanned spacecraft has a low ballistic coefficient and utilizes an auxiliary decelerating force to land. The deceleration system selected for the Viking '75 entry vehicle is a large diameter parachute. Such a parachute, together with the low ballistic coefficient of the entry vehicle, will provide the necessary aerodynamic deceleration required to traverse the Martian atmosphere and enable the spacecraft to soft land.

The selection of an aerodynamic drag-producing parachute deployed aft of a forebody requires a knowledge of the flow structure of the wake. This information is fundamental in any attempt to estimate parachute inflation-drag and -stability characteristics, drag efficiency, and structural loading. Because the flowfields behind bodies, especially blunt bodies, are extremely difficult to model analytically,[1–5] experimental tests are usually performed to provide the desired information. References 6–11 illustrate some of the studies that have been conducted to experimentally define the flow properties of wakes behind a variety of bodies. In response to initial design studies related to the Viking mission, a comprehensive wind-tunnel investigation was undertaken to measure the flowfields aft of the large-angle cone type of blunt body.[12–14] During this study, wake data were obtained for a preliminary version of the Viking '75 entry vehicle with freestream Mach numbers from 0.20 to 3.95.[15–17]

The purpose of the current paper is to summarize the experimental results in order to evaluate the characteristics of the flowfield aft of the Viking '75 entry vehicle for a wide range of freestream Mach numbers. In addition, the effects on the wake resulting from changing vehicle angle of attack are also considered.

Experimental Arrangement

The wake survey was performed using a pressure rake located aft of a model of a preliminary configuration of the Viking '75 entry vehicle (see Fig. 1). The basic component of the model was a 140° cone which had a spherical nose radius of 0.25 D in addition to a small shoulder radius at the point of maximum diameter (D). This model also had an afterbody in the base region composed of frustums of two cones. The current configuration of the Viking '75 entry vehicle has slight differences in the nose radius and afterbody section from the model used in this wake evaluation.

Two wind-tunnel facilities at the NASA Langley Research

Presented as Paper 73-475 at the AIAA 4th Aerodynamic Deceleration Systems Conference, Palm Springs, Calif., May 21–23, 1973; submitted May 14, 1973; revision received July 30, 1973.

Index categories: Jets, Wakes, and Viscid-Inviscid Flow Interactions; Viscous Nonboundary-Layer Flows.

* Aerospace Engineer. Associate Fellow AIAA.

† Aerospace Engineer. Member AIAA.

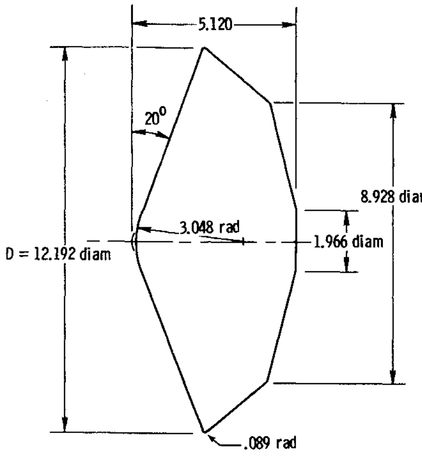

Fig. 1 Sketch of Viking entry body used in wake survey; all dimensions are presented in centimeters.

Center were used during the course of this investigation; subsonic and transonic tests were conducted in the 8-ft transonic pressure tunnel, and supersonic tests in the Unitary Plan wind tunnel. Both facilities are of the variable-pressure, continuous-flow type.

The model was mounted in the respective wind tunnels using a sting support, Fig. 2a, for the subsonic and transonic tests, and using a cantilevered wall-support strut, Fig. 2b, for the supersonic tests. Although the wall-support strut is the more desirable mounting arrangement, it was not possible to use this for the subsonic and transonic tests. There, of course, will be interference effects involved with both types of mounts, but the wall strut has the advantage of permitting pressure data to be measured along the wake center line. Care was exercised to provide symmetry in the support systems in order to avoid significant errors in the wake results. This follows the experience of Carmel and Brown[18] who observed an asymmetric wake pattern that resulted because of warpage in a wall-support strut that spanned the tunnel test section. During the supersonic tests[15] a selected amount of data were obtained aft of the cantilevered wall-support strut to assess its influence on the wake flowfield. The data showed the existence of an interference effect, but it was not large anough to alter the discussion or conclusions of the present study.

The inertial (XYZ) axis system shown in Fig. 2 is situated so that its origin is placed on the centerline of the model at the point of maximum model diameter. The longitudinal X-axis is in the direction of airflow, while the Z-axis is in the vertical direction perpendicular to X. The lateral Y-axis is perpendicular to both X and Z axes. Static and total pressures were measured in the model's wake with a pressure rake, the resulting measurements being used to calculate the various flow properties, such as M_1, V_1, and q_1. Although measurements were made throughout the wake flowfield during the experimental tests, the present paper will discuss results of data obtained only in the X-Z plane. These data cover x/D distances from 1.0 to 11.0, and z/D distances from $+1.2$ to -1.2. The reader is referred to Refs. 15–17 for detailed information concerning the wake survey locations, model description, wind-tunnel apparatus, test conditions, and accuracy of the measured data.

The Reynolds numbers for the tests varied from 4 to 14×10^6 per meter, depending on M_∞, and are within the range of values expected to be encountered during the Viking mission. Since the test Mach numbers are below those where real-gas effects are important, the wind-tunnel data obtained in air should be analogous to data obtained in a Mars environment for comparable Mach and Reynolds numbers. The test results are discussed in the following sections and provide a general description of the wake of the Viking '75 entry vehicle. These data can be used to evaluate the performance of a decelerator in the wake, a complete evaluation being dependent, of course, on the mutual interference effects between the decelerator and the wake flowfield. These interference effects could become more significant at subsonic and transonic speeds where the perturbed wake is more communicative.

Results and Discussion

Angle of Attack = 0°

Since wake dynamic pressure is an important parameter in determining parachute efficiency, the effects on the wake flowfield due to changes in M_∞, x/D, and α are assessed by examining the distribution of dynamic pressure across the wake. An example of this is shown in Fig. 3 where dynamic-pressure profiles are presented for a range of x/D locations for freestream Mach numbers of 0.6 and 2.3. It is noted that the data are essentially symmetrical about the X-axis ($z/D = 0$) which they should be with the model at $\alpha = 0°$. The differences between the dynamic pressures in the wake and in the freestream are greatest in the wake center at $x/D = 1.0$, and generally decrease as x/D or z/D increases. The wake center is defined as the locus of points in the wake where minimum dynamic pressures occur and is synonymous with the X-axis for this $\alpha = 0°$ case.

The profiles obtained in the near wake ($x/D \leqq 3$) are characterized by a region of flow reversal, by large pressure gradients (particularly in the Z-direction), and by recompression shocks at supersonic freestream Mach numbers. Measurements of zero dynamic pressure were obtained when the pressure tubes were located at the point of zero flow (rear stagnation point) or in the region of flow reversal. The region of flow

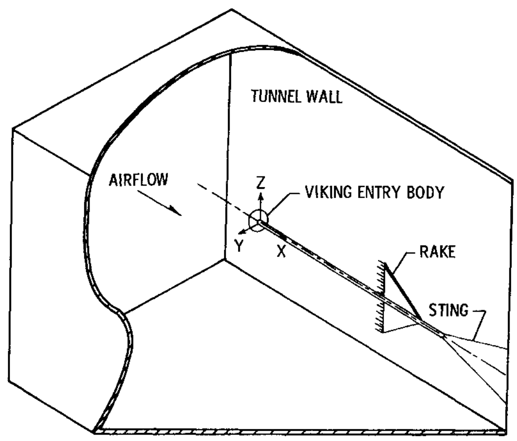

a) STING SUPPORT USED FOR SUBSONIC AND TRANSONIC TESTS

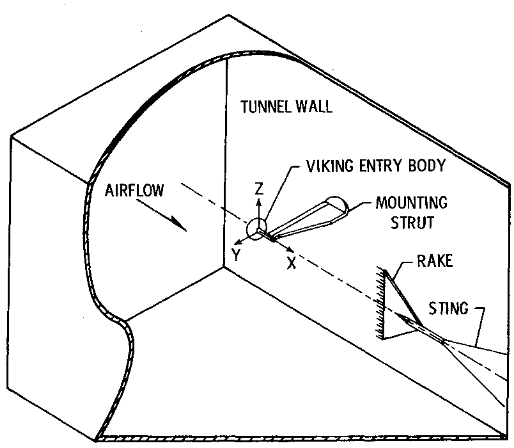

b) WALL SUPPORT STRUT USED FOR SUPERSONIC TESTS

Fig. 2 Schematic of Viking entry body mounted in tunnel.

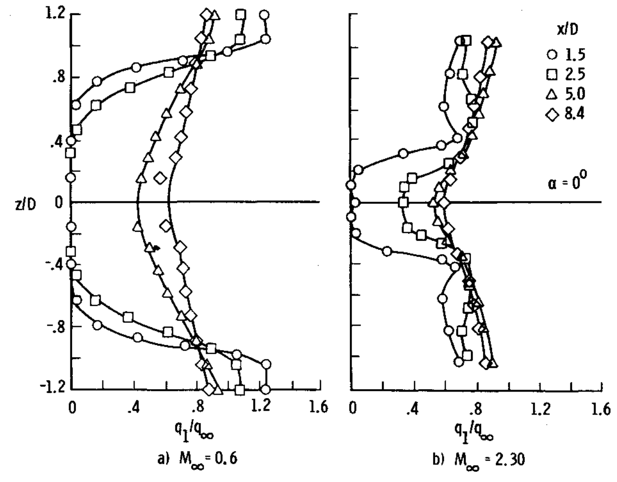

Fig. 3 Dynamic pressure profiles at longitudinal locations in wake of Viking entry vehicle for several freestream Mach numbers.

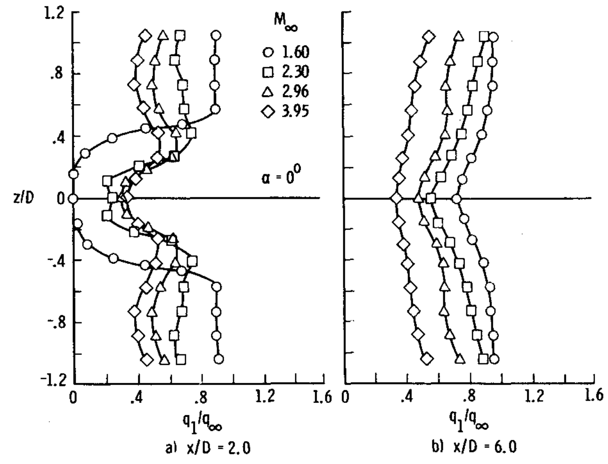

Fig. 5 Effect of supersonic M_∞ on dynamic-pressure profiles at several longitudinal locations in the wake of the Viking entry vehicle.

reversal is largest at the subsonic Mach numbers and decreases in extent as the supersonic Mach number increases. For a given profile, the large gradients in dynamic pressure occur in a region where the velocity varies from the value in the flow reversal region to the value in that part of the flow that has expanded around the shoulder of the model. Sizable dynamic-pressure gradients also can occur in the vicinity of the recompression shock, as is partially evident in the profile at $x/D = 2.5$ for $M_\infty = 2.30$, Fig. 3b. The presence of this shock becomes more obvious at higher supersonic Mach numbers.[15,16]

The dynamic-pressure profiles obtained downstream of $x/D = 3$ indicate that the flow has only small gradients along or away from the wake center and is void of any shocks. An increase in z results in an increase in dynamic pressure so that q_1 approaches q_∞ at the limits of measurement. The trends for dynamic pressure that have been discussed here are similar to those observed by McShera[8] in the wake of a cone-cylinder configuration and by Rom et al.[9] behind a two-dimensional wedge-flat-plate model.

The effects of freestream Mach number on the dynamic-pressure profiles are typified by the results shown in Figs. 4 and 5 for selected x/D locations in the wake. The data indicate that an increase in subsonic M_∞, Fig. 4, results in a corresponding decrease in q_1/q_∞ throughout the wake. At $M_\infty = 1.0$, this trend is confined to the wake center. An increase in supersonic M_∞, Fig. 5a, causes an increase in q_1/q_∞ in the flow in the near wake ($x/D \leqq 3$) close to the wake center, and causes a decrease in q_1/q_∞ in the flow toward the outer limits of measurement. At x/D locations downstream of 3, Fig. 5b, increasing the supersonic M_∞ decreases q_1/q_∞ throughout the wake.

For a planetary entry, a decelerator system (such as a parachute) is inflated at least several entry-body diameters downstream of the maximum diameter of the entry vehicle. The importance of determining the effects of x/D and M_∞ on the wake flow properties is emphasized by the realization that the decelerator must operate efficiently in a flow environment that is continuously changing as the vehicle-decelerator assembly decelerates from supersonic to subsonic speeds. An indication of the effect of M_∞ on the flow properties at the wake center may be seen in Fig. 6, where centerline dynamic-pressure and Mach number ratios are plotted for various distances downstream of the Viking entry vehicle. The effects of x/D and

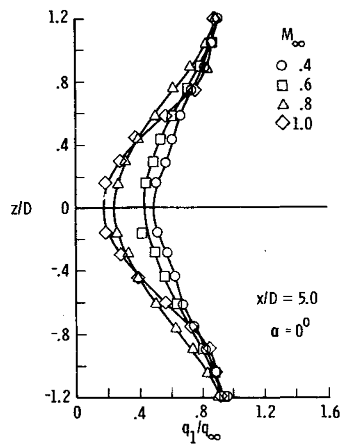

Fig. 4 Effect of subsonic M_∞ on dynamic-pressure profiles at a specific longitudinal location in the wake of the Viking entry vehicle.

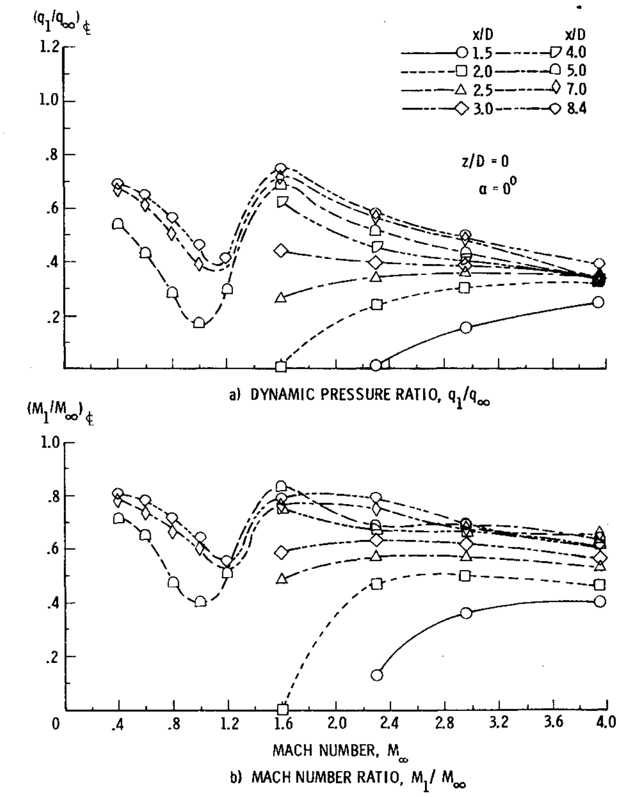

Fig. 6 Variation of wake centerline properties with freestream Mach number for Viking entry vehicle.

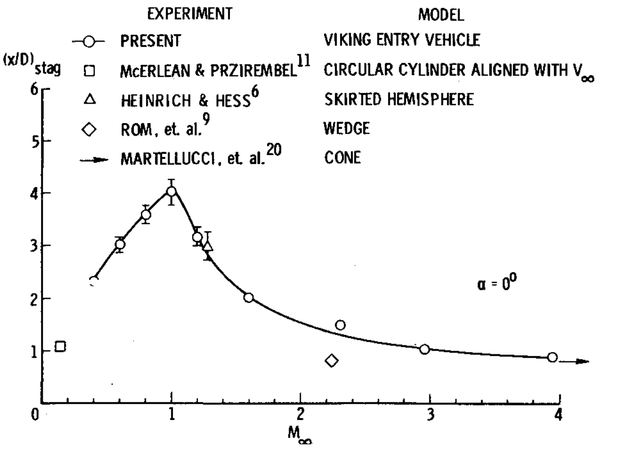

Fig. 7 Effect of freestream Mach number on location of wake stagnation point.

M_∞ on the dynamic-pressure profiles that were discussed in Figs. 3–5 are reflected in the trends of $(q_1/q_\infty)_{CL}$, Fig. 6a. One of the most pronounced effects of freestream Mach number occurs in the transonic speed range where a noticeable drop in centerline q_1/q_∞ results between $M_\infty = 1.6$ and 1.0. The decrease in $(q_1/q_\infty)_{CL}$ is approximately 75% and 47% for x/D stations 5.0 and 8.4, respectively. It is believed that these results explain, in part, the reason for the abrupt loss in parachute drag force at transonic speeds which was reported in Ref. 19. The plot of centerline Mach number, Fig. 6b, has similar trends through the transonic speed range.

Two other characteristics of the wake which are dependent on freestream Mach number are the location of the rear stagnation point and the similarity of the velocity profiles in the flowfield. These characteristics have practical application to the design of decelerator systems and are integral parts of any theoretical attempt to describe the wake. A stagnation point exists when the static and total pressures are equivalent (that is, dynamic pressure equals zero); and, in the present case, its location represents the most rearward part of the recirculation region immediately aft of the body. For $\alpha = 0°$ the stagnation point is positioned along the X-axis, its location being obtained by plotting $(q_1/q_\infty)_{CL}$ as a function of x/D for the range of test Mach numbers, and observing $(q_1/q_\infty)_{CL}$ as it approaches zero. The variation of $(x/D)_{stag}$ with freestream Mach number is presented in Fig. 7 along with measurements obtained by other investigators. McErlean and Przirembel[11] found the stagnation point to be located at $x/D = 1.08$ behind a flat-base circular cylinder aligned with an $M_\infty = 0.1$ flow. Taking this data point in conjunction with data from the present study shows that $(x/D)_{stag}$ increases with increase in subsonic M_∞ until a maximum location of about 4 is attained at the sonic condition. An increase in supersonic M_∞ causes the stagnation point to move closer to the body and eventually approach the value of $(x/D)_{stag}$ obtained by Martellucci et al.[20] at hypersonic speeds. The data suggest that the length of the recirculation region has its largest value at $M_\infty = 1$ and varies quite rapidly in the transonic speed range. These physical changes that the wake undergoes might help explain the trends of dynamic-pressure loss observed in Fig. 6a.

In an effort to determine if the velocity profiles exhibit similarity, velocity data were plotted in the usual similarity form where the velocity deficit in the wake is nondimensionalized by the maximum deficit and plotted as a function of z/b. The results are shown in Fig. 8 for two of the test Mach numbers and demonstrate a degree of similarity for the velocity profiles at subsonic and supersonic speeds. A theoretical velocity profile obtained by Goldstein[3] for an incompressible far wake is shown for reference.

Angle of Attack = 5°

An angle of attack other than 0° can occur for the type of entry vehicle considered in the present study and may be due to perturbations about the ballistic trajectory resulting from a variety of disturbances, or offset c.g. locations which allow the vehicle to fly a lifting entry. Any change in angle of attack from $\alpha = 0°$ will result in changes in the wake structure which, in turn, will influence the behavior of a decelerator (for example, parachute) system operating downstream of the vehicle. If the

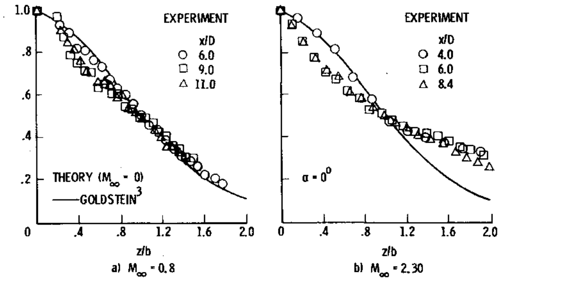

Fig. 8 Velocity distribution across the wake of the Viking entry vehicle, plotted in a form to illustrate similarity.

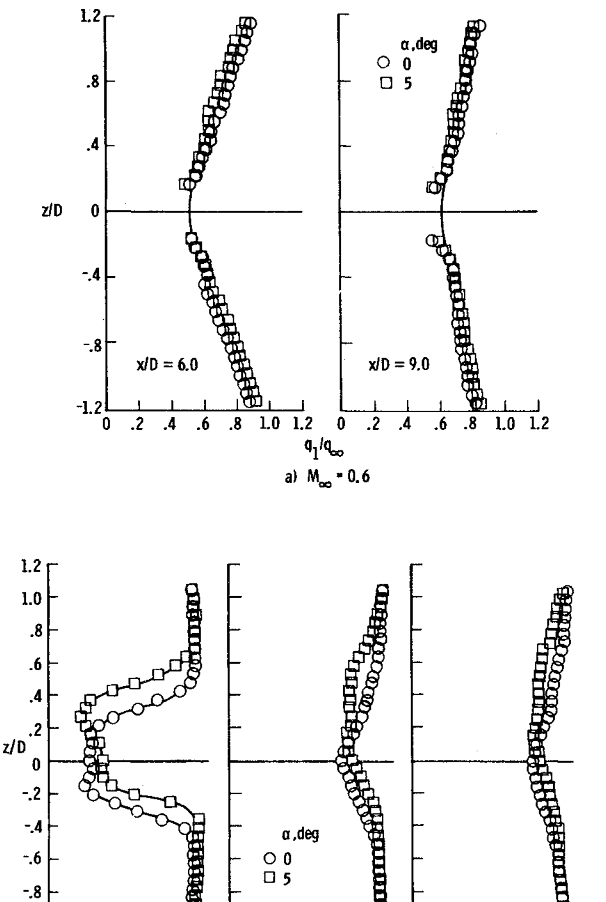

Fig. 9 Dynamic-pressure profiles behind the Viking entry vehicle at $\alpha = 0°$ and $\alpha = 5°$.

parachute is not aligned with the forebody at deployment, asymmetrical loads in the riser and bridle lines will result.

The effect of changing the angle of attack of the Viking entry vehicle model from 0° to 5° is illustrated in Fig. 9, which shows dynamic-pressure profiles for several x/D locations and two Mach numbers. The primary angle-of-attack effect is to shift the profiles away from the $\alpha = 0°$ centerline; the values of q_1/q_∞ at the wake measuring limits do not appear to be affected by the change. The shift to positive values of z occurs because the orientation of the vehicle's lift vector in the negative Z direction results in a corresponding upwash in the wake. This shift of the profiles prevailed for all locations and Mach numbers tested, although the effects of angle of attack were smallest at the largest values of x/D.

Conclusions

The importance of determining the effects of freestream Mach number M_∞ on the wake structure is emphasized by the realization that a decelerator must operate efficiently in a flow environment that is continuously changing as the vehicle-decelerator assembly decelerates from supersonic to subsonic speeds. Accordingly, an experimental investigation has been conducted to obtain the wake flow properties of a model of a preliminary configuration of the Viking '75 entry vehicle, for several model attitudes (α) and with M_∞ from 0.2 to 3.95. Efforts to evaluate the characteristics of the wake flowfield lead to the following conclusions:

1) The largest difference between the dynamic pressure in the wake (q_1) and in the freestream (q_∞) occurred at the wake center and generally decreased with increase in x/D or z/D.

2) A significant drop in the wake centerline value of q_1/q_∞ was observed in the transonic speed range, which partially explains the reason for the abrupt loss in parachute drag obtained at these speeds in previous experimental studies. This decrease in $(q_1/q_\infty)_{CL}$ coincided with a downstream shift in the location of the wake stagnation point.

3) Changing angle of attack shifted the dynamic-pressure profiles away from the $\alpha = 0°$ centerline, this shift prevailing at all x/D locations and M_∞ investigated. The angle-of-attack effect was smallest at the largest value of x/D.

4) The velocity profiles across the wake exhibited a degree of similarity at subsonic and supersonic speeds.

References

[1] Reding, J. P. and Ericsson, L. E., "Loads on Bodies in Wakes," *Journal of Spacecraft and Rockets*, Vol. 4, No. 4, April 1967, pp. 511–518.

[2] Brunner, T. W. and Nerem, R. M., "Theoretical Drag Prediction for Trailing Decelerators at Supersonic Speeds," *Journal of Aircraft*, Vol. 8, No. 12, Dec. 1971, pp. 1022–1028.

[3] Goldstein, S., "On the Velocity and Temperature Distribution in the Turbulent Wake Behind a Heated Body of Revolution," *Proceedings of the Cambridge Philosophical Society*, Vol. 34, 1938, pp. 48–67, 351–354.

[4] Lau, R. A., "Wake Analysis for Supersonic Decelerator Application. Vol. I—Theoretical Analysis and Correlation of Wind-Tunnel and Shallow-Water Tow Channel Results," CR-1543, 1970, NASA.

[5] Lau, R. A., "Wake Analysis for Supersonic Decelerator Application. Vol. II—Application of Gas-Hydraulic Analogy to Shallow-Water Tow Channel Results," CR-1544, 1970, NASA.

[6] Heinrich, H. G. and Hess, R. S., "The Velocity Pressure Distribution in the Wake of a Body of Revolution at Transonic and Supersonic Speed," Documentary Rept. ASD-TDR 63-329, May 1963, Wright-Patterson Air Force Base, Ohio, pp. 235–279.

[7] Heinrich, H. G. and Eckstrom, D. J., "Velocity Distribution in the Wake of Bodies of Revolution Based on Drag Coefficient," Documentary Rept. ASD-TDR 62-1103, Dec. 1963, Wright-Patterson Air Force Base, Ohio.

[8] McShera, J. T., Jr., "Wind-Tunnel Pressure Measurements in the Wake of a Cone-Cylinder Model at Mach Numbers of 2.30 and 4.65," TN D-2928, 1965, NASA.

[9] Rom, J., Kronzon, Y., and Seginer, A., "The Velocity, Pressure and Temperature Distribution in the Turbulent Supersonic Near Wake Behind a Two-Dimensional Wedge-Flat Plate Model," *Israel Journal of Technology*, Vol. 6, No. 1–2, 1968, pp. 84–94.

[10] Dayman, B., Jr. and Kurtz, D. W., "Forebody Effects on Drogue Drag in Supersonic Flow," *Journal of Spacecraft and Rockets*, Vol. 5, No. 11, Nov. 1968, pp. 1335–1340.

[11] McErlean, D. P. and Przirembel, C. E. G., "The Turbulent Near Wake of an Axisymmetric Body at Subsonic Speeds," AIAA Paper 70-797, Los Angeles, Calif., 1970.

[12] Campbell, J. F. and Grow, J. W., "Experimental Flow Properties in the Wake of a 120° Cone at Mach Number 2.20," TN D-5365, 1969, NASA.

[13] Brown, C. A., Jr., Campbell, J. F., and Tudor, D., "Experimental Wake Survey Behind a 120° Included-Angle Cone at Angles of Attack of 0° and 5°, Mach Numbers from 1.60 to 3.95, and Longitudinal Stations Varying from 1.0 to 8.39 Body Diameters," TM X-2139, Jan. 1971, NASA.

[14] Brown, C. A., Jr. and Campbell, J. F., "Experimental Wake Survey Behind a 140° Included-Angle Cone at Angles of Attack of 0° and 5°, Mach Numbers from 1.60 to 3.95, and Longitudinal Stations Varying from 1.0 to 8.39 Body Diameters," TM X-2409, Nov. 1971, NASA.

[15] Brown, C. A., Jr., Campbell, J. F., and Tudor, D., "Experimental Wake Survey Behind the Viking (75) Entry Body at Angles of Attack of 0° and 5°, Mach Numbers from 1.60 to 3.95, and Longitudinal Stations Varying from 1.0 to 8.39 Body Diameters," TM X-2312, Oct. 1971, NASA.

[16] Brown, C. A., Jr. and Campbell, J. F., "Evaluation of Flow Properties Behind 120°- and 140°-Included-Angle Cones and a Viking '75 Entry Vehicle at Mach Numbers from 1.60 to 3.95," TN D-7089, Jan. 1973, NASA.

[17] Brown, C. A., Jr. and Campbell, J. F., "Experimental Wake Survey Behind the Viking '75 Entry Body at Angles of Attack of 0°, 5°, and 10°, Mach Numbers from 0.2 to 1.2, and Longitudinal Stations Varying from 1.5 to 11.0 Body Diameters," TM X-2830, 1973, NASA.

[18] Carmel, M. M. and Brown, C. A., Jr., "Model Support Effects on Aerodynamic and Wake Characteristics of Large Angle Cones," *Journal of Aircraft*, Vol. 9, No. 2, Feb. 1972, pp. 99–102.

[19] Reichenau, D. E., "Aerodynamic Characteristics of Disk-Gap-Band Parachutes in the Wake of Viking Entry Forebodies at Mach Numbers from 0.2 to 2.6," AEDC TR 72-78, July 1972, Arnold Engineering Development Center, Tullahoma, Tenn.

[20] Martellucci, A., Trucco, H., Ranlet, J., and Agnone, A., "Measurements of the Turbulent Near Wake of a Cone at Mach No. 6," *AIAA Journal*, Vol. 4, No. 3, Feb. 1966, pp. 385–391.